

# Finite Temperature Nuclear Response in Extended RPA\*

Denis Lacroix<sup>a)</sup>, Philippe Chomaz<sup>a)</sup> and Sakir Ayik<sup>b)</sup>

<sup>a)</sup> *G.A.N.I.L., B.P. 5027, F-14021 Caen Cedex, France*

<sup>b)</sup> *Tennessee Technological University, Cookeville TN38505, USA*

February 9, 2008

## Abstract

The nuclear collective response at finite temperature is investigated for the first time in the quantum framework of the small amplitude limit of the extended TDHF approach, including a non-Markovian collision term. It is shown that the collision width satisfies a secular equation. By employing a Skyrme force, the isoscalar monopole, isovector dipole and isoscalar quadrupole excitations in  $^{40}\text{Ca}$  are calculated and important quantum features are pointed out. The collisional damping due to decay into incoherent 2p-2h states is small at low temperatures but increases rapidly at higher temperatures.

**PACS:** 24.30.Cz, 21.60.Jz, 25.70.Lm

**Keywords:** extended TDHF, linear response, one-body transport theory.

---

\*This work is supported in part by the U.S. DOE Grant No. DE-FG05-89ER40530.

# 1 Introduction

After discovery of giant dipole resonance in 1947, much work has been done to understand the properties of nuclear collective vibrations built on the ground state and excited states. Most of these theoretical investigations are based on the RPA theory which is quite successful in describing the mean resonance energies and fragmentation of the excitation strengths at zero and finite temperatures. However, the RPA approach, which is in fact the small amplitude limit of the TDHF theory, is not suitable for describing damping of the collective excitations [1]. Damping arises mostly by mixing of the collective state with the nearby complex states [2]. The importance of the intrinsic compound nucleus life-time has also been stressed [3, 4]. As a result of the mixing with complex states, the excitation strength spread around the mean resonance energy, and furthermore the damping width increases with the intrinsic temperature of the system as observed in giant dipole resonances in  $^{120}\text{Sn}$  [5] and  $^{208}\text{Pb}$  nuclei [6, 7, 8]. In order to describe the nuclear collective response including damping, it is necessary to go beyond the RPA theory by incorporating coupling between the collective states and the doorway configurations. There are essentially two different approaches for this purpose: (i) Coherent mechanism due to coupling with low-lying surface modes which provides an important mechanism for damping of giant resonances in particular at low temperatures [9, 4], (ii) Damping due to the coupling with incoherent 2p-2h states which is usually referred to as the collisional damping [10]. The small amplitude limit of the extended TDHF is an appropriate basis for investigating collective response, in which damping due to the incoherent 2p-2h decay is included in the form of a non-Markovian collision term [11, 12, 13]. Based on this approach, the incoherent contribution to damping at finite temperature has been calculated in Thomas-Fermi approximation in refs. [14, 15, 16]. Calculations using the Markovian limit of this semi-classical treatment, the so-called Boltzmann-Uehling-Uhlenbeck (BUU) approach, are discussed by many authors (for a review see [17]). However, as far as the collective behavior of nuclei at moderate temperature are concerned one may worry about the adequacy of semi-classical calculations which neglect most of the quantum features but the Pauli principle.

In this work, we present a first quantal investigation of the nuclear collective response at zero and finite temperatures on the extended TDHF framework in small amplitude limit, which may be referred as an extended RPA approach. In this approach, in contrast to the semi-classical treatments, the

shell effects are incorporated into the strength distributions as well as the collisional damping widths. We point out that the damping widths should be calculated by solving a secular equation. We compute the isoscalar monopole, isoscalar quadrupole and isovector dipole strength distributions in  $^{40}\text{Ca}$  at finite temperatures by employing an effective Skyrme force.

## 2 Collective response at finite temperature

In the extended TDHF theory, the evolution of the single particle density matrix  $\rho(t)$  is determined by a transport equation [16, 18, 19, 20, 21, 22, 23, 24],

$$i\hbar \frac{\partial}{\partial t} \rho - [h(\rho), \rho] = -\frac{i}{\hbar} \int_0^t d\tau \text{Tr}_2[v, G(t, t-\tau) F_{12}(t-\tau) G^\dagger(t, t-\tau)] \quad (1)$$

where  $h(\rho)$  is the mean-field Hamiltonian and the right hand side represents a non-Markovian collision term with

$$F_{12} = (1 - \rho_1)(1 - \rho_2)v\widetilde{\rho_1\rho_2} - \widetilde{\rho_1\rho_2}v(1 - \rho_1)(1 - \rho_2) \quad (2)$$

and  $G(t, t-\tau) = T \cdot \exp[-\frac{i}{\hbar} \int_{t-\tau}^t dt' h(t')]$  denotes the mean-field propagator. The small amplitude limit of the extended TDHF theory provides a suitable framework to describe collective vibrations including damping due to the coupling with incoherent 2p-2h excitations. The small deviations of the single-particle density matrix  $\delta\rho(t) = \rho(t) - \rho_0$  around a finite temperature equilibrium state  $\rho_0$  is determined by

$$i\hbar \frac{\partial}{\partial t} \delta\rho - [h_0, \delta\rho] - [\delta U + F, \rho_0] = I_0 \cdot \delta\rho \quad (3)$$

where  $\delta U = (\partial U / \partial \rho)_0 \cdot \delta\rho$  represents small deviations in the effective mean-field potential and  $F(\mathbf{r}, t) = F(\mathbf{r}) \exp(-i\omega t) + h.c.$  is a one-body excitation operator with harmonic time dependence. An explicit expression of the linearized form  $I_0 \cdot \delta\rho$  of the non-Markovian collision term can be found in a recent publication [16].

The linear response of the system to the external perturbation  $F$  is determined by expanding the small deviation  $\delta\rho(t)$  in terms of finite temperature RPA modes,

$$\delta\rho(t) = \sum_{\lambda>0} \{z_\lambda(t)\rho_\lambda^\dagger + z_\lambda^*(t)\rho_\lambda\} \quad (4)$$

where the finite temperature RPA modes,  $\rho_\lambda^\dagger$  and  $\rho_\lambda$ , are defined by

$$\hbar\omega_\lambda\rho_\lambda^\dagger - [h_0, \rho_\lambda^\dagger] - [h_\lambda^\dagger, \rho_0] = 0. \quad (5)$$

Here  $\omega_\lambda$  is the mean-frequency of the RPA mode and  $h_\lambda^\dagger = (\partial U/\partial \rho)_0 \cdot \rho_\lambda^\dagger$  represents the positive frequency part of the vibrating mean-field. It is convenient to introduce the collective operators,  $O_\lambda^\dagger$  and  $O_\lambda$ , associated with the RPA modes as  $\rho_\lambda^\dagger = [O_\lambda^\dagger, \rho_0]$  and  $\rho_\lambda = -[O_\lambda, \rho_0]$ , and they are orthonormalized according to  $Tr[O_\lambda, O_\mu^\dagger]\rho_0 = \delta_{\lambda\mu}$ . Substituting the expansion (4) and projecting by  $O_\lambda$ , we find that the amplitudes of the RPA modes execute forced harmonic motion,

$$-i\hbar\frac{d}{dt}z_\lambda + (\hbar\omega_\lambda - \frac{i}{2}\Gamma_\lambda)z_\lambda = \langle [O_\lambda, F] \rangle_0 \quad (6)$$

where  $\langle [O_\lambda, F] \rangle_0 = Tr[O_\lambda, F]\rho_0$  and  $\Gamma_\lambda$  denotes the collisional damping width of the mode. Here, we neglect a small shift of the mean frequency  $\omega_\lambda$  arising from the principle value part of the collision term. Solving this equation by Fourier transform, the response of the system to the external perturbation  $F$  can be expressed as

$$\delta\rho(\omega) = R(\omega, T) \cdot F \quad (7)$$

where  $R(\omega, T)$  denotes the finite temperature extended RPA response function including damping

$$R_{ij,kl}(\omega, T) = \sum_{\lambda>0} \left( -\frac{\langle i|\rho_\lambda^\dagger|j \rangle \langle k|\rho_\lambda|l \rangle}{\hbar\omega - \hbar\omega_\lambda + \frac{i}{2}\Gamma_\lambda} + \frac{\langle k|\rho_\lambda^\dagger|l \rangle \langle i|\rho_\lambda|j \rangle}{\hbar\omega + \hbar\omega_\lambda + \frac{i}{2}\Gamma_\lambda} \right). \quad (8)$$

The strength distribution of the RPA response is obtained by the imaginary part of the response function,

$$\begin{aligned} S(\omega, T) &= -\frac{1}{\pi} Tr\{F^\dagger Im R(\omega, T) F\} \\ &= \frac{1}{\pi} \sum_{\lambda>0} \left\{ |\langle [O_\lambda, F] \rangle_0|^2 D(\omega - \omega_\lambda) - |\langle [O_\lambda^\dagger, F] \rangle_0|^2 D(\omega + \omega_\lambda) \right\} \end{aligned} \quad (9)$$

where the sum goes over the positive frequency modes and

$$D(\omega - \omega_\lambda) = \frac{\Gamma_\lambda/2}{(\hbar\omega - \hbar\omega_\lambda)^2 + (\Gamma_\lambda/2)^2}. \quad (10)$$

The main features of the strength function are usually discussed in terms of sum rules, which are calculated from the RPA response as,

$$m_k(T) = \int_0^\infty \omega^k d\omega S(\omega, T) \quad (11)$$

However, due to the Lorentzian shape of the poles these moments are not well defined for  $k > 1$ . For a Hermitian excitation operator the energy weighted sum rule for  $k = 1$  is not effected by the damping and it is given by,

$$m_1(T) = \sum_{\lambda>0} \omega_\lambda |< [O_\lambda, F] >_0|^2. \quad (12)$$

For a multipole operator, the energy weighted sum rule leads to  $m_1(T) = \frac{1}{2} < [F^\dagger, [H, F]] >_0$  which is exactly satisfied by the finite temperature RPA sum rule, as shown by Vautherin and Vinh Mau [25].

In the Hartree-Fock basis the finite temperature RPA equation reads,

$$(\hbar\omega_\lambda - \epsilon_i + \epsilon_j) < i|O_\lambda^\dagger|j > + \sum_{l \neq k} < ik|v|jl >_A (n_l - n_k) < l|O_\lambda^\dagger|k > = 0 \quad (13)$$

where  $v = (\partial U / \partial \rho)_0$ , the indices i,j,.. represent all single particle quantum numbers including spin-isospin, and  $n_k = 1/[1 + \exp(\epsilon_k - \epsilon_F)/T]$  denotes the finite temperature Fermi-Dirac occupation numbers of the Hartree-Fock states. At zero temperature these occupation numbers are zero or one, so that the RPA operators  $O_\lambda^\dagger$ ,  $O_\lambda$  have only particle-hole and hole-particle matrix elements. At finite temperatures the RPA functions involve more configurations including particle-particle and hole-hole states. By associating a single index with the pair of indices (i,j), the RPA functions can be regarded as a vector, and in this manner eq.(13) can be expressed as an eigenvalue equation for finite temperature RPA modes [25]. According to the small amplitude limit of the extended TDHF equation, the damping width of RPA modes due to decay into incoherent 2p-2h doorway excitations is given by [16],

$$\Gamma_\lambda = \frac{1}{2} \sum | < ij|[O_\lambda, v]|kl >_A |^2 D_{ij,kl} [n_k n_l \bar{n}_i \bar{n}_j - n_i n_j \bar{n}_k \bar{n}_l] \quad (14)$$

where  $\bar{n}_i = 1 - n_i$ . In reference [16], neglecting the damping of the collective amplitude in the collision term, the energy conserving factor is taken as a sharp delta function as  $D_{ij,kl} = \text{Im}(\hbar\omega_\lambda - \epsilon_i - \epsilon_j + \epsilon_k + \epsilon_l - i\eta)^{-1}$  Here, we

take into account for depletion of the collective amplitude in the collision term by substituting  $\omega_\lambda - \frac{i}{2}\Gamma_\lambda$  in place of  $\omega_\lambda$ . Then, the factor takes a more appropriate Lorentzian form,

$$D_{ij,kl} = \frac{\Gamma_\lambda/2}{(\hbar\omega_\lambda - \epsilon_i - \epsilon_j + \epsilon_k + \epsilon_l)^2 + (\Gamma_\lambda/2)^2} \quad (15)$$

Then, expression (14) becomes a secular equation for the damping width. As we will see this self-consistency is of major importance in order to properly compute the collision width. The collective mode damps out by mixing with the intrinsic states of increasing complexity. The sequence of the complexity of the states can be classified according to the exciton number as mixing with 2p-2h, 3p-3h,  $\dots$ , Np-Nh,  $\dots$  states. The expression (14) contains only the mixing with 2p-2h doorway states in accordance with the extended TDHF theory. In order to incorporate the damping due to mixing with more complex states, the extended TDHF should be improved by including higher order correlations beyond binary collision term. The effect of the higher order mixing may be approximately taken into account by introducing an appropriate decay width,  $\Gamma_{ij,kl}$ , of 2p-2h states in the expression (15)

$$D_{ij,kl} = \frac{(\Gamma_\lambda + \Gamma_{ij,kl})/2}{(\hbar\omega_\lambda - \epsilon_i - \epsilon_j + \epsilon_k + \epsilon_l)^2 + ((\Gamma_\lambda + \Gamma_{ij,kl})/2)^2} \quad (16)$$

Then, the secular equation can also be solved considering these higher order effects.

### 3 Results

We calculate the isoscalar monopole, isoscalar quadrupole and isovector dipole excitations in  $^{40}\text{Ca}$  at several temperatures. We use the Skyrme interaction SGII for the Hartree-Fock and RPA calculations[26] and we neglect the temperature dependence of single particle energies and wave functions. We determine the hole states by solving the Hartree-Fock problem in coordinate representation. Then, the particle states are generated by diagonalizing the Hartree-Fock Hamiltonian in a large harmonic oscillator representation by including 12 major shells. In this manner, unbound continuum states are approximately included in the RPA calculations. The RPA strength distributions of the monopole  $F_0(r) = r^2$ , dipole  $F_1(\mathbf{r}) = \tau_z r Y_{10}(\hat{\mathbf{r}})$  (in isospin

symmetric systems  $N = Z$ ), and quadrupole  $F_2(\mathbf{r}) = r^2 Y_{20}(\hat{\mathbf{r}})$  excitation operators at temperatures  $T = 0, 2, 4$  MeV are shown in figure 1. As seen from the top panel of figure 1, the monopole strength at  $T = 0$  MeV exhibit a large Landau spreading over a broad energy region  $E = 16 - 28$  MeV with an average energy  $E = 21.5$  MeV. The recent experimental data also show a broad resonance around a peak value of 17.5 MeV [27]. For increasing temperature, transition strength spread a broader range towards lower energies. As shown in the middle panel, the strength distribution of isovector dipole shows a weaker temperature dependence than monopole. At  $T = 0$ , the dipole strength is concentrated at range  $E = 16 - 23$  MeV. The Landau width is large and is spreading for increasing temperature. However, the average energy of the main peak remains nearly constant around  $E = 16.5$  MeV. The experimental data shows a broad resonance at around 20 MeV [28] with a width close to 6 MeV. As illustrated at the bottom panel of figure 1, the RPA result at  $T = 0$  MeV gives a very collective quadrupole mode peaked at  $E = 17.5$  MeV, which agrees well the experimental finding of an average energy 17 MeV [29] and the calculations of Sagawa and Bertsch [30]. At higher temperatures in addition to p-h excitations, p-p and h-h excitations become possible. The p-p and h-h configurations mainly change the strength distribution at low energy side at  $E = 4$  MeV. As a result, the giant resonance has less transition strength.

Figure 2 illustrates the average energy  $\langle E \rangle = m_1/m_0$  (solid lines), and the ratios  $(m_1/m_{-1})^{1/2}$  (short dashed lines) and  $(m_3/m_1)^{1/2}$  (long dashed lines) of the monopole, dipole and quadrupole excitations as a function of temperature. The behavior of the average energy of the monopole resonance is particularly interesting, since it may be related to the compressibility coefficient of nuclear matter [31, 32].

We obtain the collisional damping widths of the collective states by calculating the expression (14) and solving the associated secular equation by graphical method. We note that the sums over single particle states needed to evaluate the expression (14), have been performed explicitly using the projection of the total spin,  $m$ , as one of the explicit quantum numbers as done in ref. [33]. Figure 3 illustrates examples of the graphical solution for giant dipole and quadrupole excitations at two temperatures  $T = 0, 2$  MeV. In this figure, the curves with dashed lines are obtained by calculating the right hand side of (14) as a function of  $\Gamma_\lambda = \Gamma_{in}$ . The intersection of this curve with the diagonal line determines the solution. The effect of the damping width

$\Gamma_{ij,kl}$  of 2p-2h states may be approximately incorporated by taking a larger value of  $\Gamma_{in}$  as indicated in eq.(16). As seen from figure 3, in most cases, the selfconsistent value of the damping width saturates very rapidly, and hence it is not modified very much by increasing  $\Gamma_{in}$ . Figure 4 shows the damping widths as a function of temperature, that are averaged over several nearby states with strengths more than 10% of the EWSR. The results for monopole, dipole and quadrupole are indicated in the top, middle and bottom panels, respectively. Collisional damping widths are generally small at low temperatures, but rapidly grow for increasing temperature. This increase appears to be more complex than the semi-classical quadratic prediction. Depending upon the mode, the increase may be linear or may saturate.

In order to understand this behavior, it is convenient to write the expression (14) of the damping width as sum over energy bins in energy  $E = \epsilon_i + \epsilon_j - \epsilon_k - \epsilon_l$  of 2p-2h states,

$$\Gamma_\lambda = \frac{1}{2} \sum_E g_{2p-2h}(E) \overline{W}_\lambda(E) D(\hbar\omega_\lambda - E) \quad (17)$$

where each bin has a small energy interval  $\Delta E$  around  $E$ , and  $D(\hbar\omega_\lambda - E)$  is the Lorentzian factor given by eq.(15). Here  $\overline{W}_\lambda(E)$  denotes the average transition rate,

$$\overline{W}_\lambda(E) = \frac{1}{g_{2p-2h}(E)} \sum_{\Delta E} | \langle ij | [O_\lambda, v] | kl \rangle_A |^2 [n_k n_l \bar{n}_i \bar{n}_j - n_i n_j \bar{n}_k \bar{n}_l]. \quad (18)$$

In this expression many terms are vanishing either due to the selection rules or due to the Pauli blocking factors. The quantity  $g_{2p-2h}(E)$  is the total number of 2p-2h states in the energy interval including only those states which are not Pauli blocked and which have non-vanishing matrix elements of the transition rate, i.e., which can be coupled to the phonon quantum numbers. Figures 5 and 6 show the density of 2p-2h states and the average transition rates as a function of the 2p-2h energy for dipole and quadrupole excitations at  $T = 0$  MeV and  $T = 3$  MeV. In dipole mode, there is no odd parity 2p-2h states available in the vicinity of the collective energy, hence the average transition rate  $\overline{W}_\lambda(E)$  and the density of states vanish at zero temperature. As a result, the collisional damping of giant dipole in  $^{40}\text{Ca}$  is zero at  $T = 0$  MeV. This behavior is a particular quantum feature due to shell effects in the extended RPA calculation of double magic light nuclei, and it can not be described in the framework of semi-classical approaches. In medium weight



and heavy nuclei, in the vicinity of the GDR strength, there are few odd parity 2p-2h configurations involving intruder states associated with the spin-orbit coupling. As a result, we expect to find a small finite damping of giant dipole resonance at zero temperature. For increasing temperature, the available phase space becomes much larger and the collisional damping of the GMR and GDR increases. This is not the case for the GQR because the increase of the phase space is compensated by a reduction of the magnitude of average transition rates. As a result, the damping width of giant quadrupole appears to saturate above  $T = 3 - 4$  MeV.

Figure 7 shows the strength distributions including the collisional damping. The giant dipole strength at  $T = 0$  MeV is smoothed by performing an averaging with a Lorentzian weight with a width of 0.5 MeV. The excitation strengths become broader for increasing temperature. The peak position of the monopole resonance does not change much, but the peak position of dipole slightly shifts down and quadrupole slightly shifts up in energy. This is a signature of the reduction of the collectivity of those states with temperature because the peak energy moves back towards the single particle expectations.

Figure 8 illustrates the FWHMs of the collective excitations at several temperatures. The widths of giant monopole and giant dipole at  $T = 0$  MeV are mainly due to fragmentation of the collective strength, i.e. the so-called Landau spreading, which is about 4 MeV in both cases. Since it is difficult to extract well defined values, the FWHM of these modes at  $T = 0$  MeV are left open in the figure. The total widths increase further by mixing of the collective mode with incoherent 2p-2h excitations at higher temperatures. However, the total width does not present the parabolic behavior predicted by semi-classical calculations.

In figure 9, long-dashed lines and solid lines show the integrated strengths over the energy interval 10 – 40 MeV as a function of temperature in the RPA and the extended RPA, respectively. As a reference, the total strength  $m_1$  is also indicated by short-dashed lines. In the RPA calculations, the modes retain a high degree of collectivity even at temperatures at  $T = 4 - 5$  MeV. However, in the extended RPA approach, as a result of damping, the excitation strength become broader and the collectivity diminishes for increasing temperature.

## 4 Conclusions

We investigate isoscalar monopole, isoscalar quadrupole and isovector dipole excitations of  $^{40}\text{Ca}$  at finite temperature in the basis of the small amplitude limit of the extended TDHF. The extended TDHF goes beyond the thermal RPA approach by including damping due to decay into incoherent 2p-2h excitations. We calculate the excitation strength distributions in a self-consistent Hartree-Fock representation by employing a Skyrme force with SGII parameters. At  $T = 0$ , the monopole and dipole strengths are fragmented and spread over a broad range because of the Landau damping, while quadrupole exhibits a single peak structure. For increasing temperature, strength in all cases becomes broader and hence the collectivity is reduced. The incoherent damping widths at low temperatures are, in general, small and thus leaving room for a possible coherence effect of doorway states in the description of the damping properties. At high temperature the collisional damping becomes large and may even dominate the spreading width since the coherence effect is expected to diminish rather rapidly. For increasing temperature, the collisional damping predicted by the quantal calculations, evolves in a more complex manner than the quadratic increase predicted by the semi-classical calculations. An interesting property of the collisional damping is that it may saturate for increasing temperature. In fact, our calculations indicate that the damping width of giant quadrupole saturates around  $T = 3 - 4$  MeV, however a saturation of the giant monopole and dipole modes is not visible at these temperatures. There are important quantal effects in the collective behavior of a hot nuclear system as illustrated in [34]. Investigations presented here, also indicates that, the quantal effects has a large influence on the damping properties of collective excitations at low temperatures, which may even persist at relatively high excitations. As illustrated in ref. [16], the magnitude of the collisional damping is rather sensitive to the effective residual interactions, for which an accurate information is not available. The effective Skyrme force is well fitted to describe the nuclear mean-field properties, but not the in-medium cross-sections and damping properties. Therefore, a systematic study of the effective interactions in this context is clearly called for. However, our investigation, while remains semi-quantitative, gives a valuable insight on the quantal properties of collective excitations at finite temperature.

### Acknowledgments

One of us (S. A.) gratefully acknowledges GANIL Laboratory for a partial support and warm hospitality extended to him during his visit to Caen. This work is supported in part by the US DOE grant No. DE-FG05-89ER40530.

### References

- [1] P. Ring and P. Schuck, *The nuclear many-body problem*, *Spring-Verlag*, New-York (1980).
- [2] G.F. Bertsch and R.A. Broglia, *Oscillation in finite quantum systems*, Cambridge (1994).
- [3] Ph. Chomaz, *Ann. Phys. Fr.* **21**(1996) 669.
- [4] W. E. Ormand, P. F. Bortignon and R. A. Broglia, *Phys. Rev. Lett.* **77** (1996) 607.
- [5] J.J. Gaardhøje, *Ann. Rev. Nucl. Part. Sci.* **42** (1992) 483.
- [6] E. Ramakrishan et al., *Phys. Rev. Lett.* **76** (1996) 2025.
- [7] E. Ramakrishan et al., *Phys. Lett.* **B383** (1996) 252.
- [8] H. J. Hofmann et al., *Nucl. Phys.* **A571** (1994) 301.
- [9] G. F. Bertsch, P.F. Bortignon and R. A. Broglia, *Rev. Mod. Phys.* **55** (1983) 287.
- [10] A. Smerzi, A. Bonasera and M. DiToro, *Phys. Rev.* **C44** (1991) 1713.
- [11] K. Ando, A. Ikeda and G. Holzwarth, *Z. Phys.* **A310** (1983) 223.
- [12] S. Ayik and M. Dworzecka, *Phys. Rev. Lett.* **54** (1985) 534; *Nucl. Phys.* **A440** (1985) 424.
- [13] P. G. Reinhard, H. L. Yadav and C. Toepfer, *Nucl. Phys.* **A458** (1986) 301.
- [14] M. Belkacem, S. Ayik and A. Bonasera, *Phys. Rev.* **C52** (1995) 2499.

- [15] S. Ayik, in *Adv. in Nuclear Dynamics* **2**, eds. W. Bauer and G. Westfall, Plenum, N.Y. (1996)
- [16] S. Ayik, O. Yilmaz, A. Gokalp and P. Schuck, Phys. Rev. **C** (1998), in press.
- [17] A. Bonasera, F. Gulminelli and J. Molitoris, Phys. Rep. **243** (1994) 1.
- [18] Y. Abe, S. Ayik, P. G. Reinhard and E. Suraud, Phys. Rep. **275** (1996) 49.
- [19] C.Y.Wong and H.H.K. Tang, Phys. Rev. Lett. **40** (1978) 1070; Phys. Rev. **C20** (1979) 1419.
- [20] S. Ayik, Z. Phys. **A298** (1980) 83.
- [21] K.Goeke and P.-G.Reinhard, "*Time-Dependent Hartree-Fock and Beyond*", Proceedings, Bad Honnef, Germany (1982).
- [22] R. Balian, Y. Alhassid, and H. Reinhardt, Phys. Rep. **131** (1986) 1.
- [23] C.Y. Wong and K.T.R. Davies, Phys. Rev. **C28** (1983) 240.
- [24] M. Tohayama, Nucl. Phys. **A437** (1985) 443; M. Tohayama, Phys. Rev. **C36** (1987) 187.
- [25] D. Vautherin and N. Vinh Mau, Phys. Lett. **B120** (1983) 261; Nucl. Phys. **A422** (1984) 140.
- [26] N. Van Giai and H. Sagawa, Nucl. Phys. **A371** (1981) 1.
- [27] D. H. Youngblood, Y.-W. Lui and H. L. Clark, Phys. Rev. **C55** (1997) 2811.
- [28] B. L. Berman and F. C. Fultz, Rev. Mod. Phys. **47** (1975) 713.
- [29] A. van der Woude *et al.*, Contrib. Florence Intern. Conf. on Nuclear Structure (1983) p. 241.
- [30] H. Sagawa and G.F. Bertsch, Phys. Lett. **B146** (1984) 138.
- [31] J.P. Blaizot, Phys. Rep. **64** (1980) 171.

- [32] J.Treiner, H.Krivine and O. Bohigas, Nucl. Phys. **A371** (1981) 253.
- [33] F. Catara, Ph. Chomaz and N. Van Giai, Phys. Lett. 233B (1989) 6.
- [34] D. Lacroix and Ph. Chomaz, Nucl. Phys. **A** (1998)-*in press*.

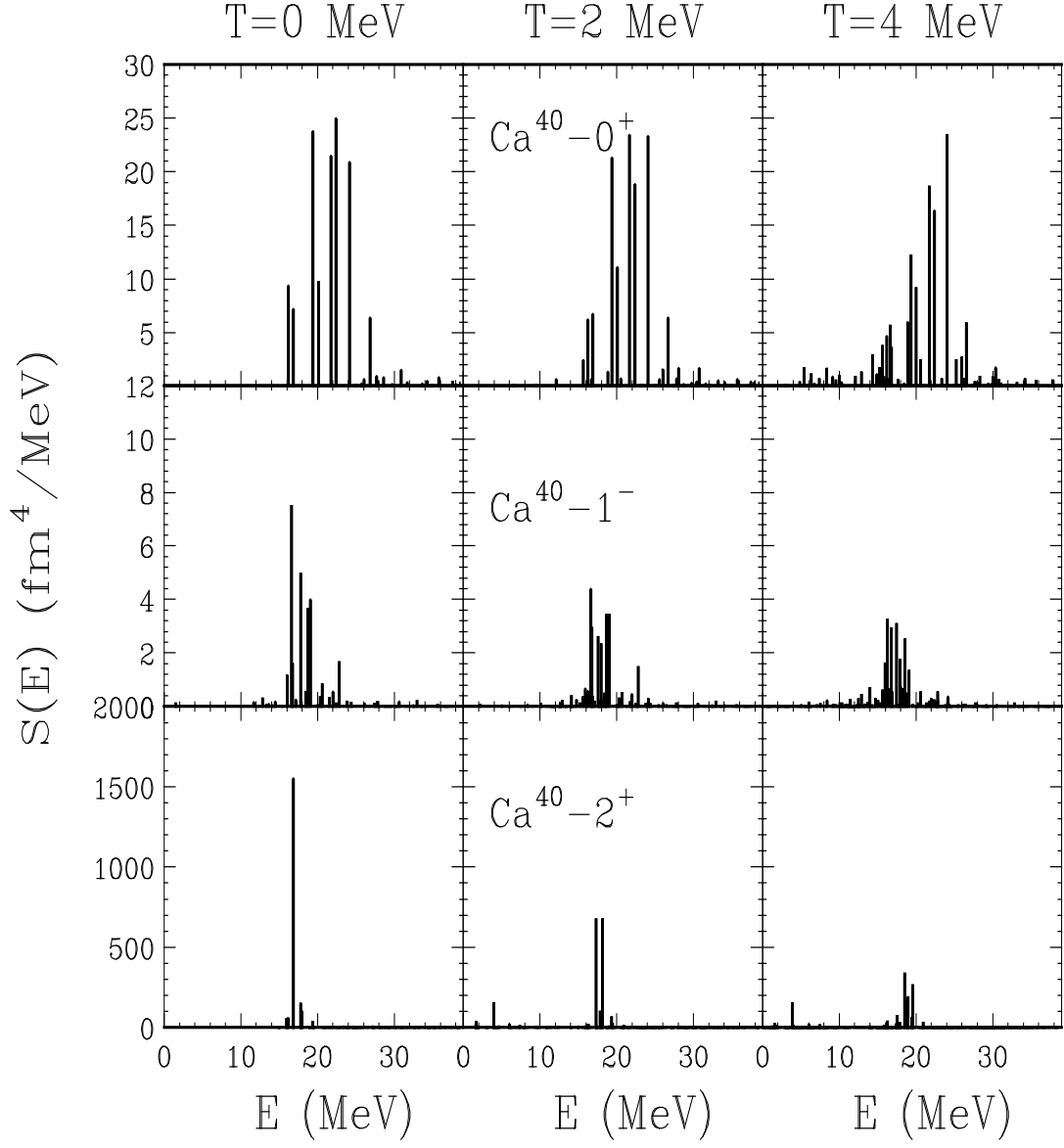


Figure 1: RPA strength distributions in  $\text{Ca}^{40}$  as a function of the energy at temperatures  $T = 0, 2, 4$  MeV for isoscalar monopole  $0^+$  (top), isovector dipole  $1^-$  (middle) and isoscalar quadrupole  $2^+$  (bottom) excitations.

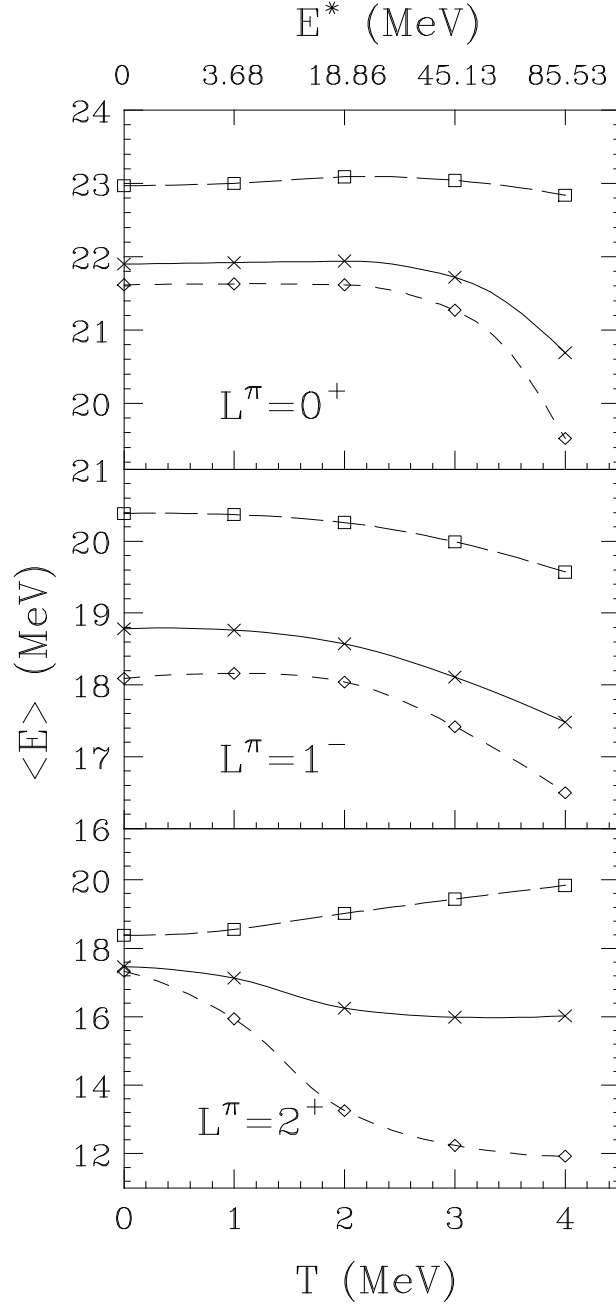


Figure 2: Averaged energy of the monopole, dipole and quadrupole excitations in  $^{40}\text{Ca}$   $m_1/m_0$  (solid line) and the moment ratios  $(m_1/m_{-1})^{1/2}$  (short dashed line) and  $(m_3/m_1)^{1/2}$  (long dashed line) as a function of the temperature.

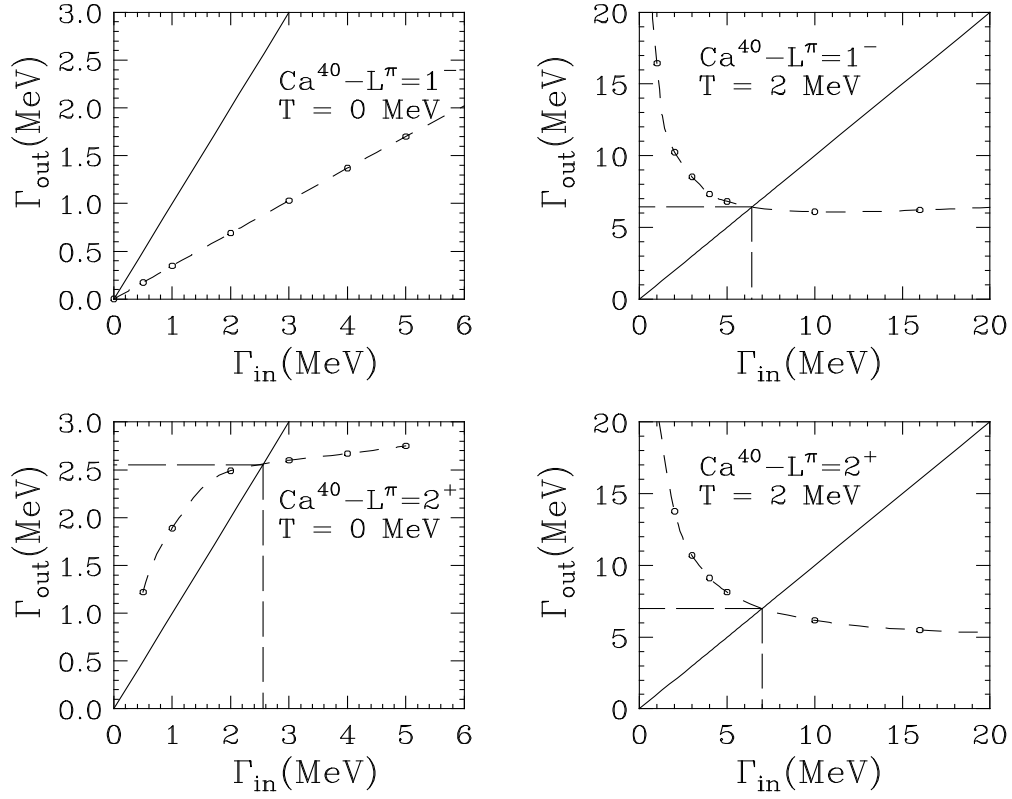


Figure 3: Graphical solution of the secular equation for the damping width for  $L^\pi = 1^-$  (top)  $L^\pi = 2^+$  (bottom) at  $T=0$  MeV (left) and  $T=2$  MeV (right).



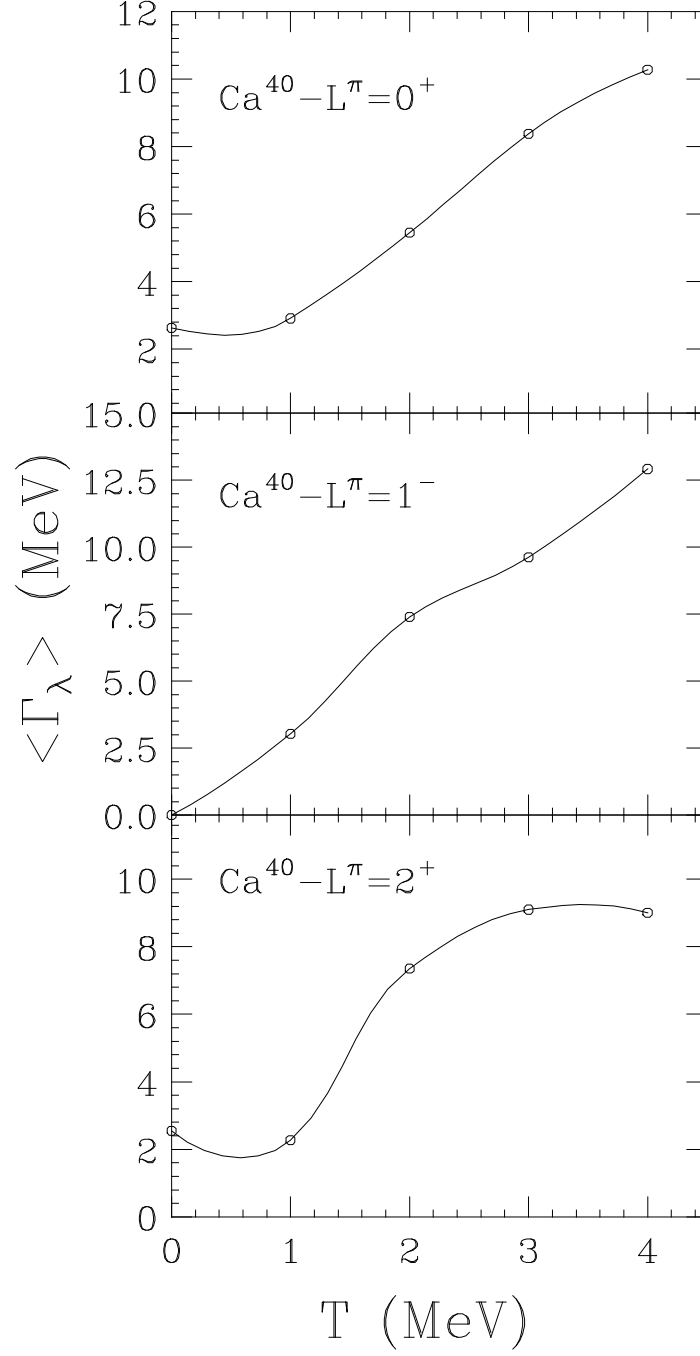


Figure 4: Collisional damping widths that are averaged over nearby states with more than 10% of the EWSR,<sup>17</sup> for monopole, dipole and quadrupole modes as a function of temperature.

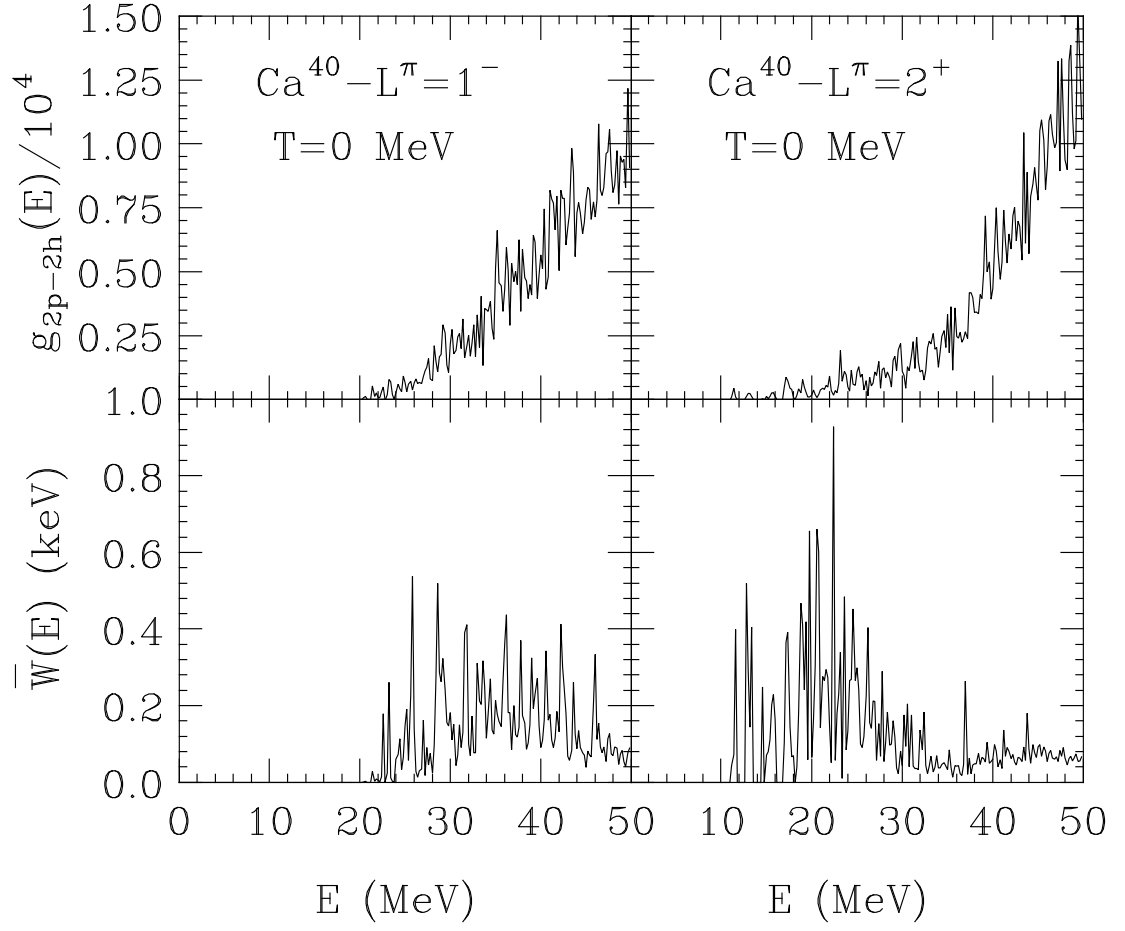


Figure 5: Top: Energy dependence of the density of 2p-2h states  $g_{2p-2h}$  for  $L^\pi=1^-$ (left) and  $L^\pi=2^+$  (right) at zero temperature. Bottom: Averaged transition rate between collective states and 2p-2h states as a function of the energy of  $2p-2h$  states.

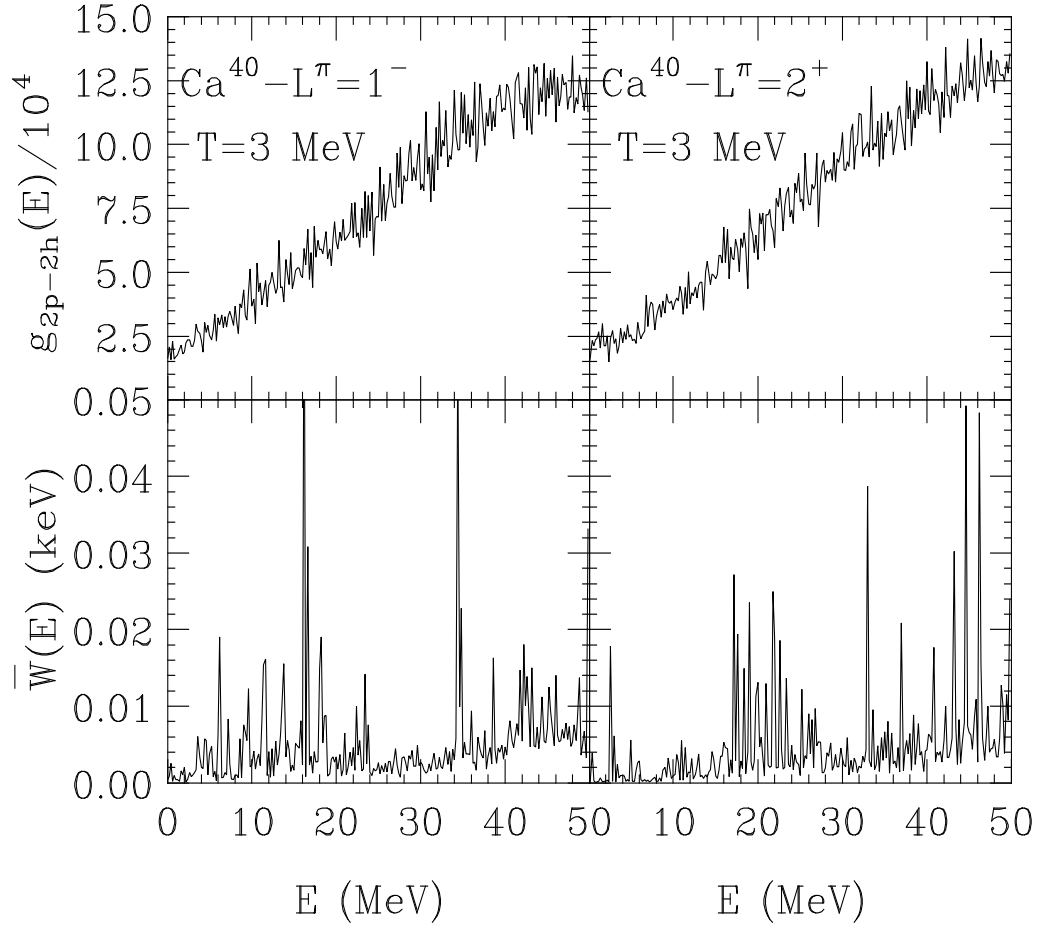


Figure 6: The same as in figure 5, but at  $T = 3$  MeV.

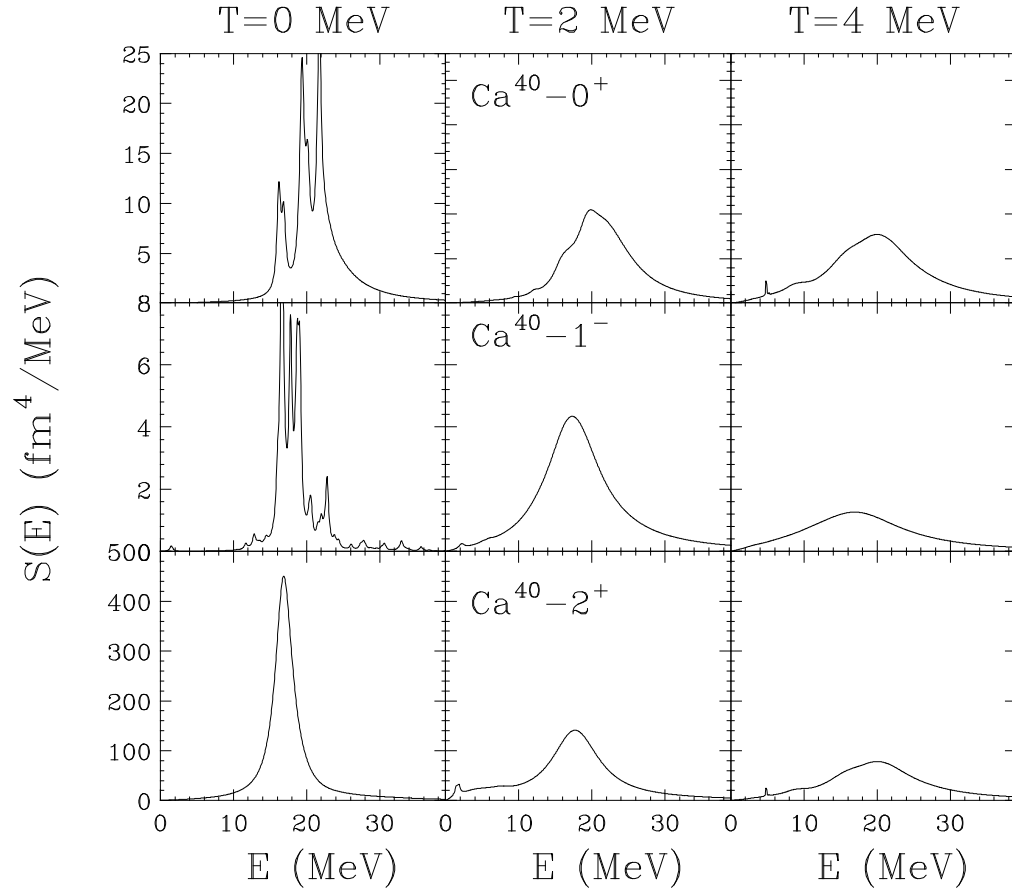


Figure 7: The extended RPA strength distributions of the monopole, dipole and quadrupole excitations as a function of temperature.

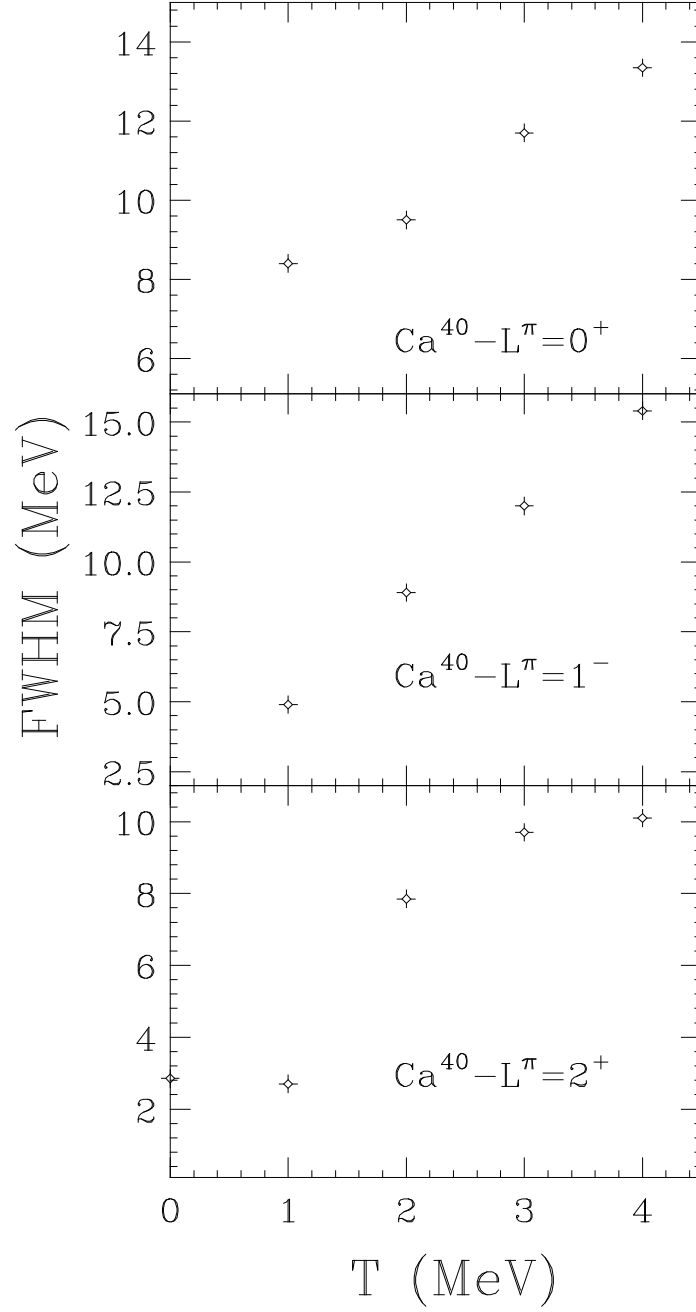


Figure 8: The full widths at half maximum of the strength distributions at several temperatures.

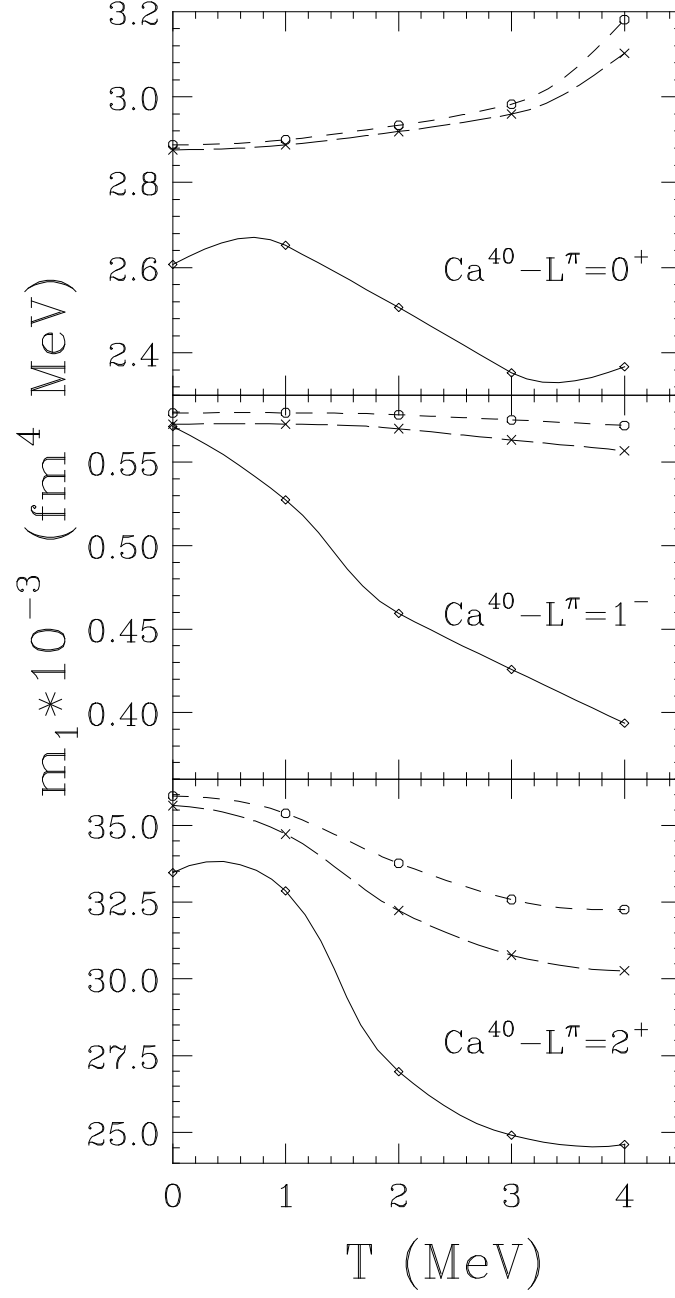


Figure 9: Integrated strengths over the energy interval 10 – 40 MeV in the RPA (long-dashed line) and the extended RPA (solid line). The total strengths  $m_1$  are plotted as a reference by short dashed lines.